

Studying Galaxy Clusters Using The Sunyaev-Zel'dovich Effect

M.Sc. Thesis

*Submitted in partial fulfillment of the
requirements for the awards of the degree
of
Master of Science*

by

Himanshu



Department of Astronomy, Astrophysics and Space Engineering

INDIAN INSTITUTE OF TECHNOLOGY INDORE

June 12, 2021



Suman Majumdar

INDIAN INSTITUTE OF TECHNOLOGY INDORE

CANDIDATE'S DECLARATION

I hereby certify that the work which is being presented in the thesis entitled “**Studying Galaxy Clusters Using The Sunyaev-Zel'dovich Effect**” in the partial fulfillment of the requirements for the award of the degree of **Master of Science** and submitted in the **Discipline of Astronomy, Astrophysics and Space Engineering, Indian Institute of Technology Indore**, is an authentic record of my own work carried out during the time period from August,2020 to June,2021 under the supervision of **Dr Siddharth Malu**(Associate Professor, IIT Indore) and **Dr Abhirup Datta**(Associate Professor, IIT Indore) .

The matter presented in this thesis has not been submitted by me for the award of any other degree of this or any other institute.


8 June 2021

**Signature of the student with date
(Himanshu)**

This is to certify that the above statement made by the candidate is correct to the best of our knowledge.


10/06/2021
Signature of the Supervisor 1 of
M.Sc. thesis (with date)
(Dr Siddharth Malu)


10/06/2021
Signature of the Supervisor 2 of
M.Sc. thesis (with date)
(Dr Abhirup Datta)

Himanshu has successfully given her M.Sc. Oral Examination held on **8th June,2021**.


Signature(s) of Supervisor(s) of MSc thesis
Date: 10/06/2021


Signature of Convener, DPGC
Date:


Signature of M.Sc. coordinator
Date: 10-06-2021


Signature of Head of Department
Date: 10/06/2021

Saptarshi Ghosh

Signature of PSPC Member 1
Date: 10/06/2021

Manoneeta Chakraborty

Signature of PSPC member 2
Date: 10/06/2021

Suman Majumdar
10/06/2021

Signature of PSPC Member 3
Date:

ACKNOWLEDGEMENTS

This project has taken significant time and effort to complete, yet it has been a fantastic journey for me while working on this project for about a year. Not only did it teach me something new, but it also enabled me to draw out results. This report takes on a lot of work from the research community. I want to express my sincere gratitude to my supervisors **Dr Siddharth Malu** and **Dr Abhirup Datta**, for guiding me toward this topic, "Studying galaxy clusters using the Sunyaev-Zel'dovich effect ", and providing me with the necessary knowledge and support that enabled me to get satisfactory results. Last but not least, I would like to thank my parents, friends and colleagues for their motivation and constant support.

Abstract

A well-known way to study clusters of galaxies is the Inverse-Comptonization of Cosmic Microwave Background(CMB) photons by Intra-Cluster medium(ICM), popularly known as Sunyaev-Zel'dovich effect(SZE). For hot ICM gas, relativistic effects must be taken into account. In this work, we have used SZpack¹, a numerical library takes into account of these effects and allows high-speed and accurate calculations of SZ signals(0.001% at frequencies $\approx 1000\text{GHz}$) up to high temperatures($\gtrsim 75\text{KeV}$). We have simulated SZ flux maps of galaxy clusters with a given morphology of thermal electron population and temperature, in order to compare them with actual observations made in cm-wave range using the current generation of radio telescopes. The combination of these simulations and observed data will allow the mapping of pressure in the ICM, which is especially useful for studying the dynamics of cluster mergers

¹www.jb.man/SZpack

Contents

List of Figures	i
1 Introduction	1
1.1 Motivation:SZ effect as a tool to probe cluster physics	1
1.2 Thesis Organization	2
2 Thermal and Kinetic SZ Effect	3
2.1 Physics of the SZ Effect	3
2.1.1 Thermal SZ Effect	3
2.1.2 The kinetic SZ effect (kSZ)	3
2.2 Representation of thermal SZ signals	4
2.2.1 Computing the SZ signal for hot and fast moving galaxy clusters	5
2.2.2 SZ signals for continuous temperature and electron population profiles	6
2.2.3 SZ signal for a two-temperature plasma	7
2.3 Impact of bandwidth on SZ spectrum	7
2.4 Results:	8
2.4.1 Simulation of thermal SZ signals for different cluster models	8
2.4.2 SZ signal for isothermal clusters	8
2.4.3 SZ signal for non-isothermal cluster	10
3 Non-Thermal SZ Effect	12
3.1 Exact Total SZ Effect	13
3.2 Approximation of Non-Thermal SZ distortion	14
3.3 Results:	16
3.4 Impact of ntSZ on total SZ	16
4 SZ parameter estimation	19
4.1 Data	19
4.2 Models	19

4.2.1	Asymptotic Model:	19
4.2.1.1	Results:	20
4.2.2	Two-Temperature Model:	21
4.2.2.1	Results:	21
4.3	Non-Thermal parameter estimation	22
5	Conclusions and Future Prospects	25
5.1	Thermal SZ simulations of Bullet cluster:	25
5.1.1	Simulated tSZ map:	27

List of Figures

2.1	Figure from Mroczkowski et al. 2019 showing how CMB photons interact with thermal electrons and the energy of up-scattered photon would be higher in its direction and vice-versa.	4
2.2	Figure from Mroczkowski et al. 2019 showing the up-scattering of incoming photon when it interacts with hot plasma electron characterized by a bulk velocity	4
2.3	Figure from Chluba, Nagai, et al. 2012 showing the kinematic distortions with cluster temperature $\theta_e = 0.05$, bulk velocity $\beta_c = 0.01$ and direction $\mu_c = 1, 0$, noting the higher order kinematic effect than just the dipole term.	6
2.4	First and second derivatives w.r.t frequency , where the second order derivative represents the correction term that arises due to frequency resolution.(cf., Chluba, Switzer, et al. 2013)	8
2.5	Projection of electron density according to Isothermal β -model	9
2.6	Projection of Compton- y according to Isothermal β -model.	9
2.7	Projection of SZ intensity(ΔI) in MJy at two different frequencies for $T_e = 14KeV$	10
2.8	Projection of temperature for a non-isothermal cluster following a β model	11
2.9	Projection of Compton- y for a non-isothermal cluster.	11
2.10	Projection of frequency for which SZ signal peaks for a non-isothermal cluster	11
2.11	Projection of SZ signal (ΔI) for frequency map given in fig. 2.10 using SZpack numerical library.	11
3.1	Impact of non-thermal pressure on total SZ in Bullet cluster ,image from Lage et al. 2014	13
3.2	Integrated non-thermal pressure using eq. 3.12	16
3.3	Calculation only in diagonally significant region	16
3.4	Spectral features of ntSZ (by plotting $\tilde{g}(x)$), thSZ and kSZ, each effect is multiplied by a certain factor to match the magnitude for comparison.	17

3.5	Thermal SZ map from simulated X-ray data at 170GHz	17
3.6	ntSZ map at 170 GHz using same values of p_1, A, B and γ as in 4.4	17
4.1	Left: Posterior distribution for Prokhorov's model after running the MCMC. Right: Best fit according to Prokhorov's model with 95 % confidence interval shown.	20
4.2	Poor representation of SZ signals using asymptotic approach, similar to Prokhorov's model.	21
4.3	Left: Posterior distribution for model parameters for two-temperature model(cf., Chluba, Switzer, et al. 2013), on x-axis we have τ, f_τ and T_e . Right: Best model fit for two-temperature model.	22
4.4	Relativistic optical-depth τ_{rel}	23
4.5	Calculations only in diagonally significant region	23
4.6	Total SZ signals at different frequencies	24
5.1	Temperature map from X-Ray observations	26
5.2	Optical depth τ from eq. 5.1	26
5.3	Simulated SZ signals for bullet cluster at frequencies from upper left to right 18,33,100 and 750 GHz respectively.	27
5.4	SZ map at 100 GHz with X-Ray temperature contours shown	28
5.5	SZ observation of bullet cluster from Di Mascolo, Luca et al. 2019 at 100GHz	28

Chapter 1

Introduction

The possibility of distortion (spectral and spatial) in the most energetic Planckian radiation field (Cosmic Microwave Background) aroused ever since the discovery of the radiation by [Penzias et al. 1965](#). The Comptonization of these CMB photons by hot electron in ICM called Sunyaev-Zel'dovich effect which is complementary to the X-Ray studies of the cluster of galaxies provides a unique and independent cosmological probe. Calculations of this distortion by hot ICM plasma were first calculated years ago ([Y. B. Zeldovich et al. 1969](#)). The theory and significance of this process were extensively discussed in [Sunyaev and Y. B. Zeldovich 1970](#), [Birkinshaw 1999](#), [Rephaeli 1995a](#) and more recently by [Mroczkowski et al. 2019](#).

1.1 Motivation: SZ effect as a tool to probe cluster physics

Galaxy cluster being the largest structures present in the observable universe provides important constraints on the cosmological parameters such as Hubble's constant and that is why it is of cosmological interest in studying these structures.

The integrated thermal pressure can be directly obtained from SZ signals of galaxy clusters ($\frac{\Delta T_{SZE}}{T_{CMB}} \propto \int n_e T_e dl$), hence it serves as a critical tool to probe cluster and IC plasma physics.

Since SZ distortion is not a function of red-shift therefore it renders it as a critical tool in probing ICM gas dynamics at high red-shift cosmos where along with X-Ray studies, ICM gas parameters and the integrated pressure profile can be constrained.

1.2 Thesis Organization

In chapter 2, a review of how to calculate SZ distortions produced by a thermal population of electrons is given and concluded with simulation of thermal SZ intensity maps for various cluster types; chapter 3 will discuss the non-thermal SZ effect and its importance concluding with the mixing of different SZ effects and its effect on total SZ signal. In chapter 4, we will demonstrate the use of SZpack by redoing the analysis done by [Chluba, Switzer, et al. 2013](#) and also we will prepare non-thermal SZ maps at different frequencies that can be used for parameter estimation just as in the case of the thermal SZ effect. In chapter 5, the application of simulations done so far, to bullet cluster, is concluded by preparing the thermal SZ distortion map for bullet cluster and comparing it with the actual interferometric observation of thermal SZ across the bullet cluster shock.

Chapter 2

Thermal and Kinetic SZ Effect

2.1 Physics of the SZ Effect

The CMB photons when passes through the hot dense plasma that is found in the clusters of galaxies gets scattered and gains or loses energy in the line of sight of the cluster, this can be easily understood realizing that in the frame of reference of CMB when electron are at rest they produces no net effect, as the photon number is conserved. However, when electron are moving they can transfer some of their energy to the CMB photons and thereby changing the whole spectrum. Therefore the it is the distribution of electrons that governs the outgoing spectrum of CMB photons imparting the distortion that varies with frequency.

2.1.1 Thermal SZ Effect

When the dynamics of electrons is described by an isotropic (relativistic) Maxwell-Boltzmann distribution(thermal electrons),and photons gets up-scattered by these thermal electrons this gives rise to the so-called thermal SZ (tSZ) effect.

2.1.2 The kinetic SZ effect (kSZ)

When the cluster moves as a whole with a bulk velocity with respect to the CMB rest frame, it will see a natural dipole term for the scattered CMB radiation as first deduced by [Sunyaev and Y. B. Zeldovich 1972](#), this dipole term produces is what is defined as kinetic SZ effect that purely depends upon whether there is an angle between cluster's bulk velocity and the CMB frame. Using relativistic transformation, see [Sunyaev and I. B. Zeldovich 1980](#) the distortion due to this bulk motion of cluster can be obtained.

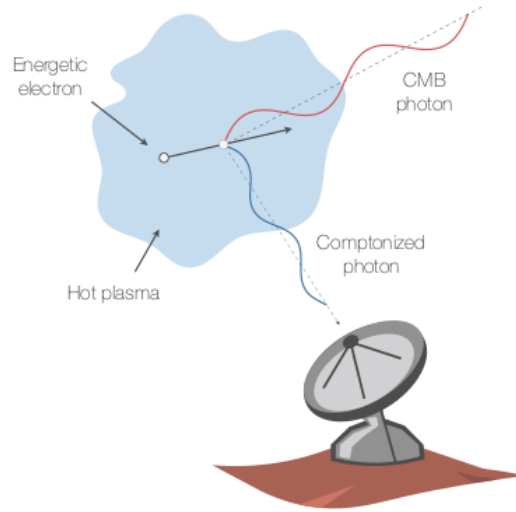


Figure 2.1: Figure from [Mroczkowski et al. 2019](#) showing how CMB photons interact with thermal electrons and the energy of up-scattered photon would be higher in its direction and vice-versa.

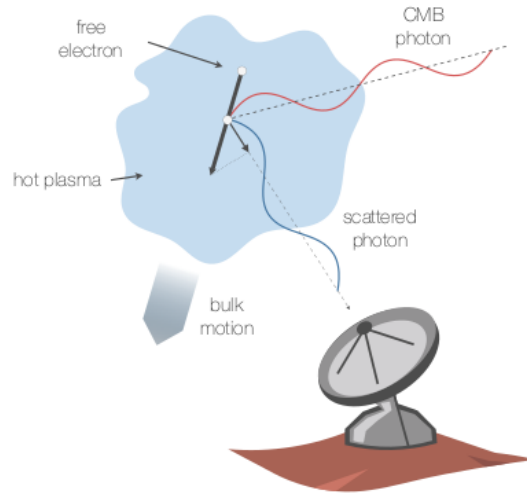


Figure 2.2: Figure from [Mroczkowski et al. 2019](#) showing the up-scattering of incoming photon when it interacts with hot plasma electron characterized by a bulk velocity

2.2 Representation of thermal SZ signals

At high temperature plasma dynamics of ICM gas it is important to represent SZ signals accurately as earlier concluded and approached by ([Rephaeli 1995b](#); [Challinor et al. 1998](#); [Itoh et al. 1998](#); [Sazonov](#)

et al. 1998 using a Taylor series approximation. However at cluster bulk velocities as high as ($v \approx 1000 \text{Kms}^{-1}$) and temperature greater than $kTe \geq 10 \text{keV}$ the Taylor series approximation fails and to solve this problem a new approach was developed in Chluba, Nagai, et al. 2012 and Chluba, Switzer, et al. 2013 that we discuss briefly.

2.2.1 Computing the SZ signal for hot and fast moving galaxy clusters

In this work we use the formulation developed in Chluba, Switzer, et al. 2013 in which the disentanglement between frequency dependent function and spatial function that decides the SZ distortion is done and applied in the form of SZpack library that can run on a standard laptop to calculate the distortion in a few seconds.

SZpack allows fast and precise computation of the SZ signal for hot, moving clusters of galaxies. The signal can be defined using line of sight temperature and velocity moment described as below:

$$\begin{aligned} y^{(k)} &= \int \theta_e^{k+1} d\tau, & b_0^{(k)} &= \int \beta_c^2 \theta_e^k d\tau \\ b_1^{(k)} &= \int \beta_c P_1(\mu_c) \theta_e^k d\tau, & b_2^{(k)} &= \int \beta_c^2 P_2(\mu_c) \theta_e^k d\tau \end{aligned} \quad (2.1)$$

Where $y^{(k)}$ is now the generalised compton-y parameter that dictates the thermal SZ, θ_e is the temperature, P_1 and P_2 are Legendre polynomial, μ_c and $d\tau$ are cluster velocity and optical depth along line of sight respectively. Now we can write full relativistically correct SZE as a simple multiplication of the set of these moment with the spectral functions.

$$tSZ(\Delta I) = F * m \quad (2.2)$$

where m is the set of spatial function in 2.1 and F is the spectral function. This formulation takes care of the kinematic signals as well, as shown in fig. 2.3 Calculation in SZpack are done by neglecting polarization effects and in single scattering approximation with a Maxwell–Jüttner distribution of electrons.

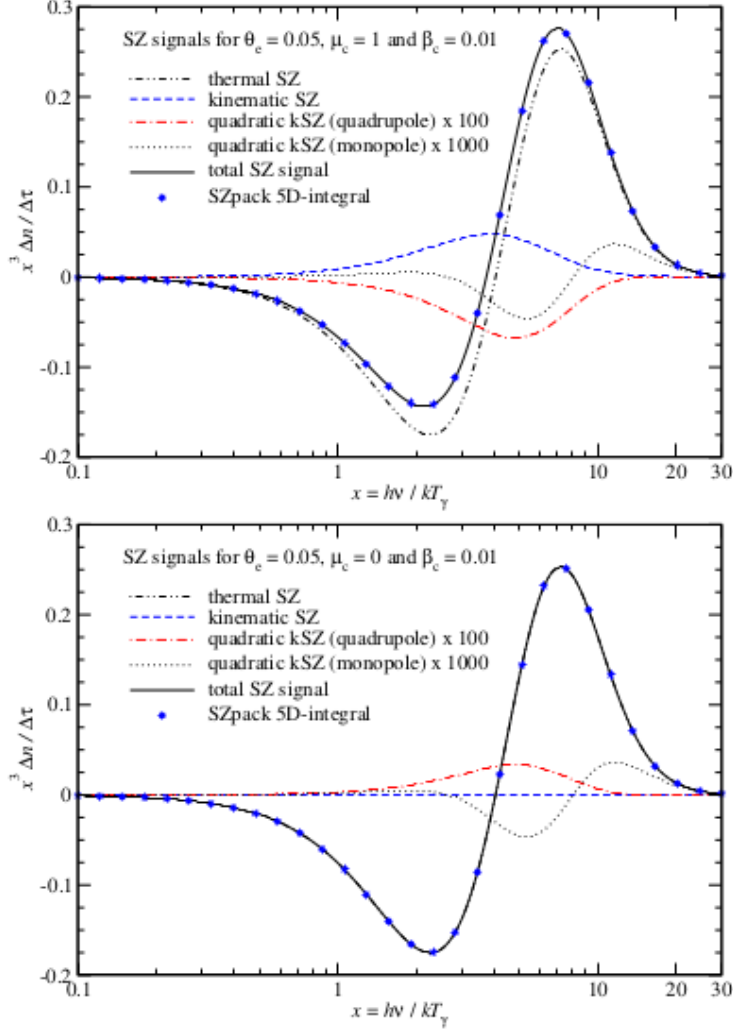


Figure 2.3: Figure from [Chluba, Nagai, et al. 2012](#) showing the kinematic distortions with cluster temperature $\theta_e = 0.05$, bulk velocity $\beta_c = 0.01$ and direction $\mu_c = 1, 0$, noting the higher order kinematic effect than just the dipole term.

2.2.2 SZ signals for continuous temperature and electron population profiles

As described in [Chluba, Switzer, et al. 2013](#) we can estimate SZ signals for electron density and temperature that varies smoothly by expanding the moments around some average velocity, optical depth and average temperature.

By defining $T_{e,SZ}(\hat{y}) = (m_e c^2 / k) y^{(0)} / y^{(-1)} = \tau^{-1} \int T_e d\tau$ and for velocity components $\beta_{c,\parallel} = \beta_c \mu_c$ and $\beta_{c,\perp} = \beta_c \sqrt{1 - \mu_c^2}$ of the moving volume element, we can similarly define

$\beta_{c,\parallel,SZ} = \tau^{-1} \int \beta_{c,\parallel} d\tau$ and since the SZ signal is only sensitive to $\beta_{c,\perp,SZ}^2 = \tau^{-1} \int \beta_{c,\perp}^2 d\tau$, but not $\beta_{c,\perp,SZ}$ directly.

Expanding around $\tau, T_{e,SZ}, \beta_{c,\parallel,SZ}$, and $\beta_{c,\perp,SZ} = 0$, the mean SZ signal takes the form

$$S \approx S_{\text{iso}}^{(0)} + S_{\text{iso}}^{(2)} \omega^{(1)} + C_{\text{iso}}^{(1)} \sigma^{(1)} + D_{\text{iso}}^{(2)} \kappa^{(1)} + E_{\text{iso}}^{(2)} \beta_{\text{c},\perp,\text{SZ}}^2 + \dots \quad (2.3)$$

Where the signal vectors and dispersion variables are

$$\begin{aligned} \mathbf{C}_{\text{iso}}^{(k)} &= (k!m!)^{-1} \theta_{\text{e},\text{SZ}}^k \partial_{\theta_{\text{e},\text{SZ}}}^k \partial_{\beta_{\text{c},\parallel,\text{SZ}}} \mathcal{S}_{\text{iso}}(\tau, T_{\text{e},\text{SZ}}, \beta_{\text{c},\parallel,\text{SZ}}, \beta_{\text{c},\perp,\text{SZ}}) \\ \mathbf{D}_{\text{iso}}^{(k)} &= (k!)^{-1} \partial_{\beta_{\text{c},\parallel,\text{SZ}}}^k \mathcal{S}_{\text{iso}}(\tau, T_{\text{e},\text{SZ}}, \beta_{\text{c},\parallel,\text{SZ}}, \beta_{\text{c},\perp,\text{SZ}}) \\ \mathbf{E}_{\text{iso}}^{(k)} &= (k!)^{-1} \partial_{\beta_{\text{c},\perp,\text{SZ}}}^k \mathcal{S}_{\text{iso}}(\tau, T_{\text{e},\text{SZ}}, \beta_{\text{c},\parallel,\text{SZ}}, \beta_{\text{c},\perp,\text{SZ}}) \\ \kappa^{(k)} &= \tau^{-1} \int (\beta_{\text{c},\parallel} - \beta_{\text{c},\parallel,\text{SZ}})^{k+1} d\tau \\ \sigma^{(k)} &= \left(T_{\text{e},\text{SZ}}^k \tau \right)^{-1} \int (T_{\text{e}} - T_{\text{e},\text{SZ}})^k (\beta_{\text{c},\parallel} - \beta_{\text{c},\parallel,\text{SZ}}) d\tau \end{aligned} \quad (2.4)$$

This boils down the parameter estimation problem for SZ signals to constraining the set of parameters that describes the ICM gas, these parameters are $\mathbf{p} = \left(\tau, T_{\text{e},\text{SZ}}, \beta_{\text{c},\parallel,\text{SZ}}, \omega^{(1)}, \sigma^{(1)}, \kappa^{(1)}, \beta_{\text{c},\perp,\text{SZ}}^2 \right)$.

2.2.3 SZ signal for a two-temperature plasma

A two-temperature plasma model for cluster can be described as follows:

If we have plasma at two different temperature in separate region of space in cluster atmosphere then we can take temperature in one region to be $T_{e,1} = T_e$ and a high temperature region to be at $T_{e,2} = T_e(1 + \Delta)$, where Δ is temperature difference in these region.

Then we can specify separate optical depths as well as, $\tau_1 = \tau(1 - f_\tau)$ and $\tau_2 = f_\tau * \tau$, where τ is the total optical depth. And we can now define average SZ weighted temperature and the deviations in temperatures as,

$$\begin{aligned} T_{\text{e},\text{SZ}} &= T_e (1 + f_\tau \Delta) \\ \omega^{(1)} &= f_\tau \frac{(1-f_\tau)\Delta^2}{(1+f_\tau\Delta)^2} \\ \omega^{(2)} &= f_\tau \frac{(1-f_\tau)(1-2f_\tau)\Delta^3}{(1+f_\tau\Delta)^3} \end{aligned} \quad (2.5)$$

Later we will use this model in constraining these parameters and if they non-zero that would suggest the plasma present in cluster contains two temperature.

2.3 Impact of bandwidth on SZ spectrum

As formulated in [Chluba, Switzer, et al. 2013](#) the effect of frequency resolution can be calculated if we define the average frequency \bar{x} and dispersion $\sigma_x^2 = \overline{x^2} - \bar{x}^2$ over the filter, to lowest order we have, $\bar{S} \approx S_{\text{iso}}(\bar{x}) + \frac{1}{2} \partial_{\bar{x}}^2 S_{\text{iso}}(\bar{x}) \sigma_x^2$. In figure 2.5 we show the first and second order derivatives w.r.t frequency,

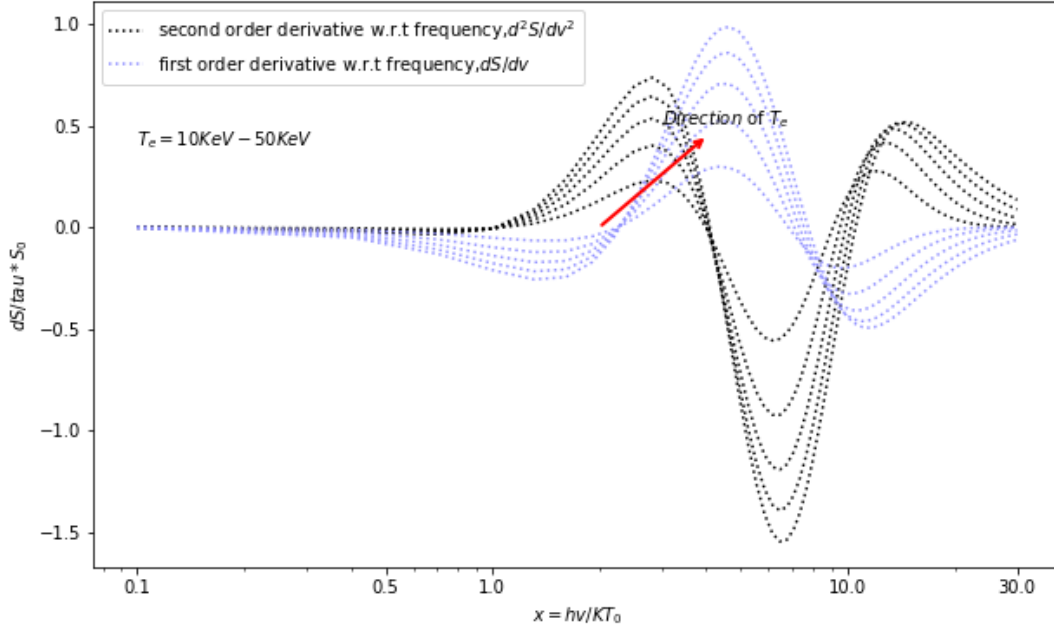


Figure 2.4: First and second derivatives w.r.t frequency , where the second order derivative represents the correction term that arises due to frequency resolution.(cf.,[Chluba, Switzer, et al. 2013](#))

2.4 Results:

2.4.1 Simulation of thermal SZ signals for different cluster models

Here we demonstrate the use of SZpack for simulating SZ maps given some electron density profile and temperature profile. In reality these profile can be obtained by fitting X-Ray observations with models. And usually what is done is a complimentary X-Ray and SZ study of galaxy clusters.

2.4.2 SZ signal for isothermal clusters

Model:

We use the simple isothermal- β -model([Cavaliere et al. 1978](#)) for modelling of temperature profile and electron density profile that then we can integrate to obtain a map of thermal optical depth map, this optical depth map and temperature then defines our observational parameters that will go in SZpack functions to calculate the distorted radiation in MJy/Sr.

$$N_e = N_{e,0} [1 + (r/r_c)^2]^{-3\beta/2} \quad \text{and} \quad T_e \equiv \text{const} \quad (2.6)$$

For a typical cluster e.g. Coma like cluster, using $N_{e,0} \approx 10^{-3} \text{ cm}^{-3}$ as the central density of electron profile and for cluster core radius using $r_c \approx 100 \text{ kpc}$, and $\beta \approx 2/3$. Here we are assuming that cluster does not have any bulk velocity therefore the SZ morphology will be entirely depend upon optical depth ($\tau(\hat{\gamma})$) and temperature map given.

Simulation results:

Here we make projections by integrating the electron density in small region of space and thereby obtain the corresponding compton-y and prepare the SZ projections in these regions to get the final results as shown in figures below.

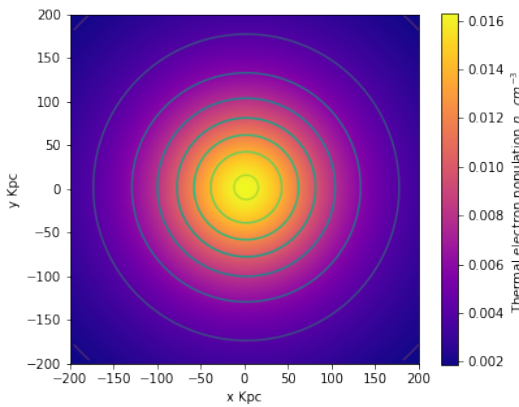


Figure 2.5: Projection of electron density according to Isothermal β -model

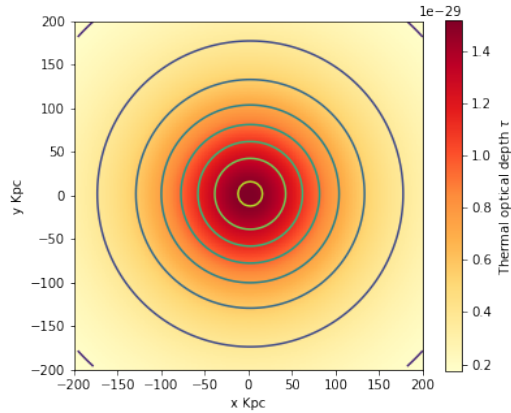


Figure 2.6: Projection of Compton-y according to Isothermal β -model.

Using a constant temperature of $T_e = 14 \text{ KeV}$ for iso-thermal cluster SZ maps are obtained as shown in 2.7

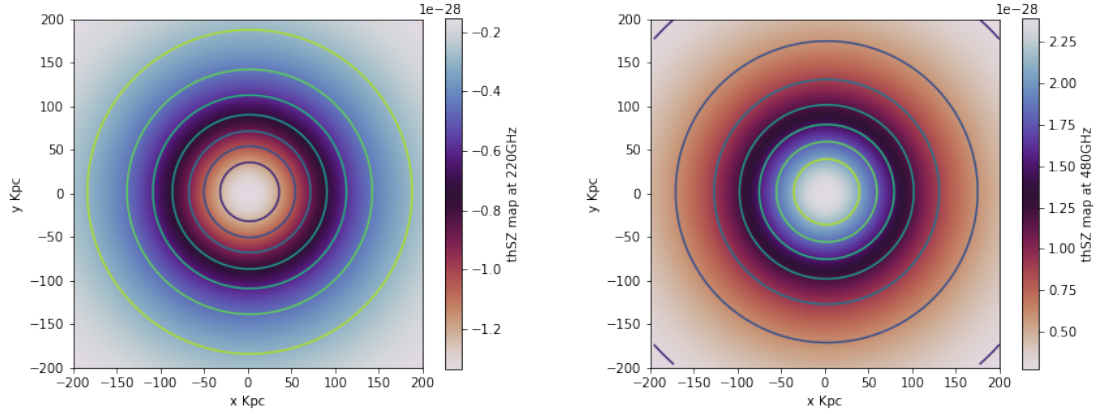


Figure 2.7: Projection of SZ intensity(ΔI) in MJy at two different frequencies for $T_e = 14KeV$

In figure 3.3 the frequency used is such that at which SZ signal peaks which remains a constant since for constant temperature peak signal remains the same.

2.4.3 SZ signal for non-isothermal cluster

For such cluster we have used the same variation of temperature as the isothermal β -model to illustrate that such projections can be made where the temperature varies.

From the expression 2.1 we can easily notice that the cluster morphology depends upon temperature and as soon as it is not a constant it cannot be taken out of the integral for generalized Compton- y , and here we show this fact by simulating SZ maps for a given spatial varying temperature map, as we show in simulations below.

each small regions of space the temperature is calculated assuming it follows the same isothermal β -model variation.

In fig. 2.9 we have used electron density profile as same as above, however as the temperature varies in each region of space the SZ signal varies and is calculated using SZpack for different frequencies and the peak SZ signal is found for each such frequency in a particular region of space, as we show in figures below.

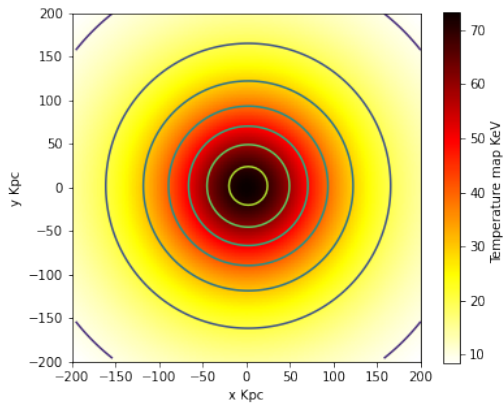


Figure 2.8: Projection of temperature for a non-isothermal cluster following a β model

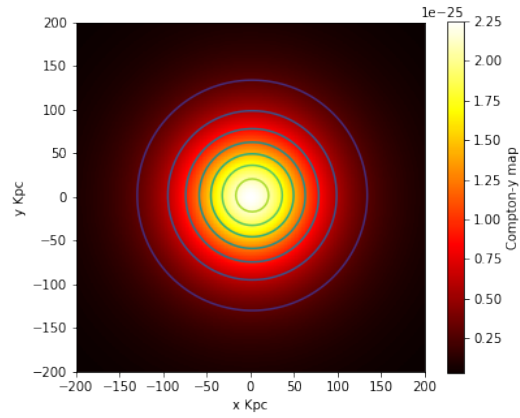


Figure 2.9: Projection of Compton- y for a non-isothermal cluster.

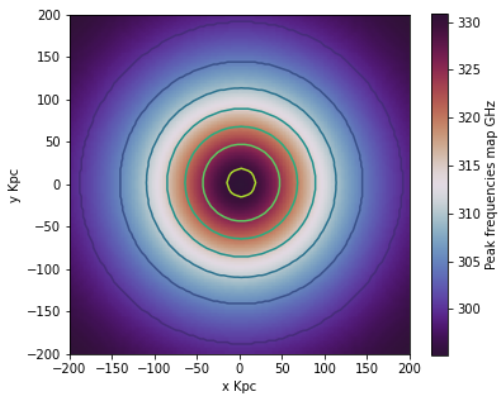


Figure 2.10: Projection of frequency for which SZ signal peaks for a non-isothermal cluster

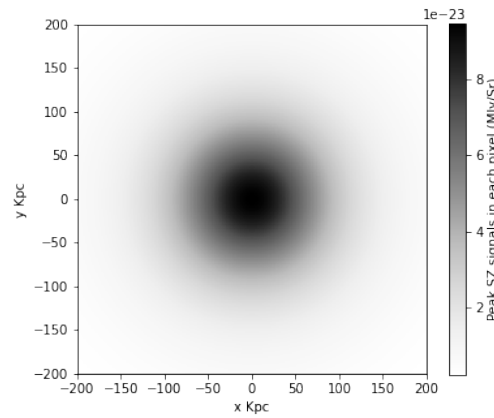


Figure 2.11: Projection of SZ signal (ΔI) for frequency map given in fig. 2.10 using SZpack numerical library.

Chapter 3

Non-Thermal SZ Effect

We discussed and computed SZ maps assuming scattering from only single thermal population of electrons in the cluster environment, however the real situation is far more complicated and what we have is a mixture of different electron population. Due to scattering from the convoluted thermal and non-thermal population, what we get is the contamination in the thermal SZ effect. In general due to scattering from this convoluted distribution of electron population it is challenging to disentangle these effects from the total SZ intensity map without certain approximations see [3.2](#). The non-thermal SZ (ntSZ) signals provides us with a way to probe the cluster dynamics related to high energy phenomenons like shocks, cluster merger events, AGN etc., that are proposed to be responsible for non-thermal injection of electrons see [Arnaud 2008](#) for a review of non-thermal emission in clusters of galaxies. For the origin and physics of these non-thermal electron population injection that impacts large scale structure formation see [Brunetti et al. 2014](#), [Bykov et al. 2019](#) and references therein.

An excellent example of a merging system is the bullet clusters of galaxies, for which if non-thermal pressure support was not accounted in Magneto-Hydrodynamic (MHD) simulation study by [Lage et al. 2014](#), it lead to minor inconsistencies in X-Ray observations but huge discrepancy between SZ observations and simulated model ([3.1](#)), making it a perfect verified source of non-thermal electron population in the cluster atmosphere and to conduct such SZ simulation studies.

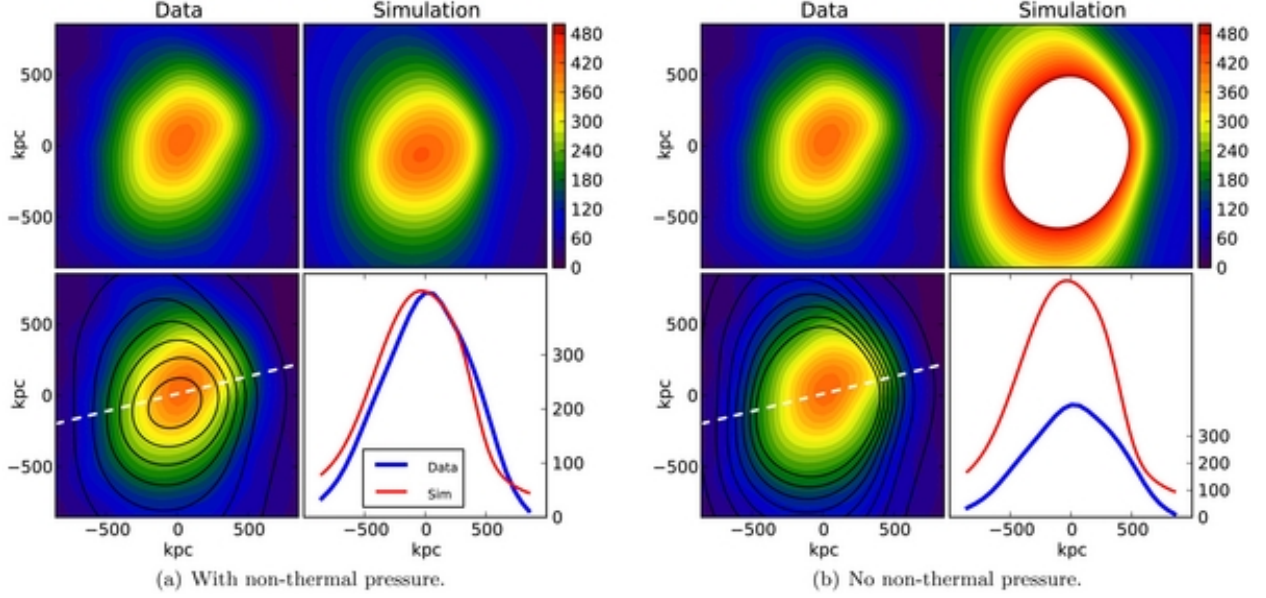


Figure 3.1: Impact of non-thermal pressure on total SZ in Bullet cluster ,image from [Lage et al. 2014](#)

While theoretical progress has been made in computing the ntSZ accurately (e.g.,[Colafrancesco et al. 2002](#),[Palladino et al. 2002](#)) the observational aspects have been quite challenging; for the first unambiguous detection of ntSZ in a radio galaxy jet/lobe see [Malu et al. 2017](#).

We will now calculate ntSZ signals for a non-thermal electron distribution defined by a single power law which is the characteristic of synchrotron energy spectrum. The energetics of this spectrum is determined by a natural low energy cut-off called p_{min} ([O'Dell et al. 1970](#),[Malu et al. 2017](#)). By preparing ntSZ maps at different frequencies the non-thermal pressure profile and p_{min} can be inferred and constrained more accurately when compared with the observations. Such an inference on integrated pressure profile and p_{min} which is directly related to magnetic fields in the ICM of galaxy clusters, will help in more accurate description and origin of such magnetic fields at high red-shifts (see, [Govoni and Feretti 2004](#) for a review on cluster magnetic fields,[Govoni, Murgia, et al. 2006](#) for a specific example on Abell 2255). We will conclude with the simulations of total SZ maps assuming the linear combination model for thermal and non-thermal contributions in single scattering approximation.

3.1 Exact Total SZ Effect

In general situation is complex as discussed in the beginning of the chapter and eq.3.14 no longer approximates the total signal well. The probability that a CMB photons gets scattered by, with a

frequency shift $s = \log(\frac{\nu'}{\nu})$ is given by [Enßlin et al. 2000](#),

$$P_1(s) = \int_0^{\infty} dp f_e(p) P_s(s; p) \quad (3.1)$$

$P_s(s; p)$ is defined in eq.3.6 Then,the spectrum of scattered CMB photons is then given by,

$$I(x) = \int_{-\infty}^{+\infty} ds I_0(xe^{-s}) P(s) \quad (3.2)$$

Where, $I_0(x) = 2 \frac{(k_B T_0)^3}{(hc)^2} \frac{x^3}{e^x - 1}$ is the incident spectrum of photons, and $x = h\nu / K T_{CMB}$ is the dimensionless frequency parameter.

The probability $P_{tot}(s)$ of scattering from a mix population of electron is given by the convolution of the respective probability functions in eq. 3.1 as([Colafrancesco et al. 2002](#)),

$$P_{tot}(s) = P_A(s) \otimes P_B(s). \quad (3.3)$$

The exact spectral distortion produced by two electron populations on the CMB radiation is given by:

$$I_{tot}(x) = \int_{-\infty}^{+\infty} I_0(xe^{-s}) P_{tot}(s) ds \quad (3.4)$$

3.2 Approximation of Non-Thermal SZ distortion

Distortion in CMB intensity due to a normalised electron distribution $f(p)$, where p is the dimensionless electron momentum(i.e., $p = p_{phys}/m_e c$) in first order in optical depth can be represented as([Mroczkowski et al. 2019](#)),

$$\Delta I_\nu \approx I_0 x^3 \tau_{rel} \int_0^{\infty} f(p) p^2 dp \int_{-s_m(p)}^{s_m(p)} P(s, p) [n_{bb}(xe^s) - n_{bb}(x)] ds \quad (3.5)$$

Where $n_{bb} = 1/(e^x - 1)$, and maximal logarithmic energy shift, $s_m(p) = \ln[(1 + \beta)/(1 - \beta)]$ with $\beta(p) = p/\sqrt{1 + p^2}$. The scattering kernel, $P(s, p)$, is given by(e.g,[Rephaeli 1995a](#))

$$P(s, p) = \frac{3}{8} \left\{ \frac{e^s(1+e^s)}{p^5} \left[\frac{3+2p^2}{2p} (|s| - s_m) + \frac{3+3p^2+p^4}{\sqrt{1+p^2}} \right] - \frac{|1-e^s|}{4p^6} [1 + (10 + 8p^2 + 4p^4) e^s + e^{2s}] \right\} \quad (3.6)$$

We will use single power law distribution for $f(p)$ i.e.,

$$f_{e,rel}(p; p_1, p_2) = \frac{(\alpha - 1)}{p_1^{1-\alpha} - p_2^{1-\alpha}} p^{-\alpha} \quad (3.7)$$

Where $p_1 < p < p_2$ and α is spectral index and can be found from radio halo studies of galaxy clusters for e.g see [Pizzo et al. 2009](#), [Feretti, L. et al. 2001](#), [Vacca, V. et al. 2014](#). And throughout this work we will take $\alpha = 2.5$ which is consistent with synchrotron-radio spectra of many clusters.

In eq. 3.5 we have replaced the optical depth with relativistic optical depth τ_{rel} which is related to integrated non-thermal pressure as,

$$\tau_{rel} = \frac{\sigma_T}{\langle K_B T_e \rangle} \int P_{rel} dl \quad (3.8)$$

Now the spatial features of ntSZ are captured by eq.3.8 Where the term $\langle K_B T_e \rangle$ is given by([Colafrancesco et al. 2002](#)),

$$\langle K_B T_e \rangle = \int_0^\infty dp f_e(p) \frac{1}{3} p v(p) m_e c \quad (3.9)$$

And for a single power law this term is evaluated to be,

$$\langle K_B T_e \rangle = \frac{m_e c^2 (\alpha - 1)}{6 [p^{1-\alpha}]_{p_2}^{p_1}} \left[B_{\frac{1}{1+p^2}} \left(\frac{\alpha - 2}{2}, \frac{3 - \alpha}{2} \right) \right]_{p_2}^{p_1} \quad (3.10)$$

And the frequency dependent term can written separately as,

$$\tilde{g}(x) = I_0 x^3 \int_0^\infty f(p) p^2 dp \int_{-s_m(p)}^{s_m(p)} P(s, p) [n_{bb}(xe^s) - n_{bb}(x)] ds \quad (3.11)$$

Therefore for single electron population there is a direct separation between frequency dependent and spatially varying functions, however both these function are connected by the low energy cut-off p_{min} for non-thermal distribution thereby allowing better constraints on it if the analysis uses a two-dimensional approach. However instead of using the whole SZ map we can use the most significant line of data realising cluster symmetry and reduce the dimensionality of the problem for MCMC analysis and saving the computational cost.

For instance we have calculated the spatial term i.e integrated non-thermal pressure using a fitting function that is red-shift and mass independent, given by [Nelson et al. 2014](#),

$$\frac{P_{rand}}{P_{total}}(r) = 1 - A \left\{ 1 + \exp \left[- \left(\frac{r/r_{200m}}{B} \right)^\gamma \right] \right\} \quad (3.12)$$

Where P_{rand} is the non-thermal pressure and $P_{total} = P_{th} + P_{rand}$, $P_{th} = \int n_e(l) K_B T_e(l) dl$ is the thermal pressure. Now the ntSZ distortion can be represented more conveniently as ,

$$\Delta I_\nu \approx \tau_{rel} * \tilde{g}(x) \quad (3.13)$$

3.3 Results:

Using eq. 3.12 we have first numerically calculated the integral by writing our own code in python then this will be an input in accordance with eq.3.13, we separately then wrote codes for numerically computing the spectral features defined by eq. 3.11 and calculated the non-thermal distortion profile for $A = 0.5, B = 0.8, \gamma = 1.5$ taking $r_{200m} = 150kpc$ as halo radius, throughout we will use the same values for simulation of ntSZ.

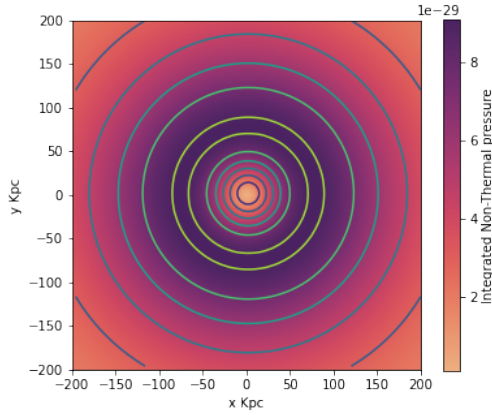


Figure 3.2: Integrated non-thermal pressure using eq. 3.12

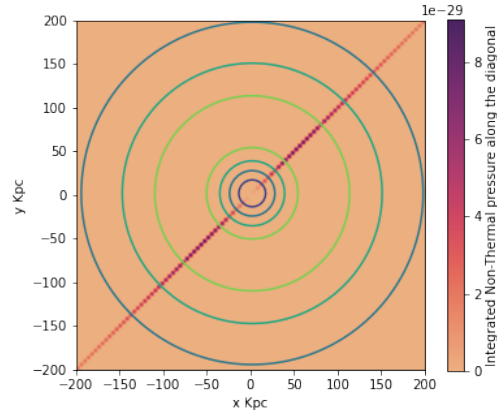


Figure 3.3: Calculation only in diagonally significant region

3.4 Impact of ntSZ on total SZ

Here we show the impact of ntSZ on total SZ both spectral and spatial. The entanglement of various SZ effect can be clearly seen in fig. 3.4

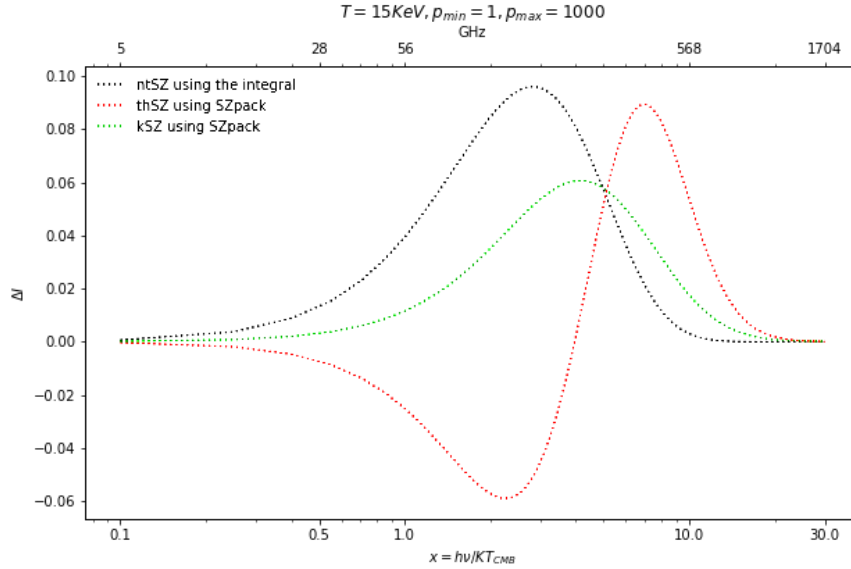


Figure 3.4: Spectral features of ntSZ (by plotting $\tilde{g}(x)$), thSZ and kSZ, each effect is multiplied by a certain factor to match the magnitude for comparison.

From fig.3.4 we can also see that a multi-wavelength study of SZ effect is necessary to filter these various components out from the total effect.

Assuming the electron density and temperature maps from X-Ray observations we have compared the thSZ map and ntSZ map as shown below.

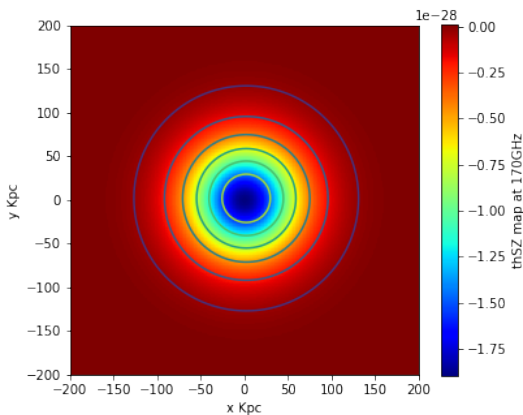


Figure 3.5: Thermal SZ map from simulated X-ray data at 170GHz

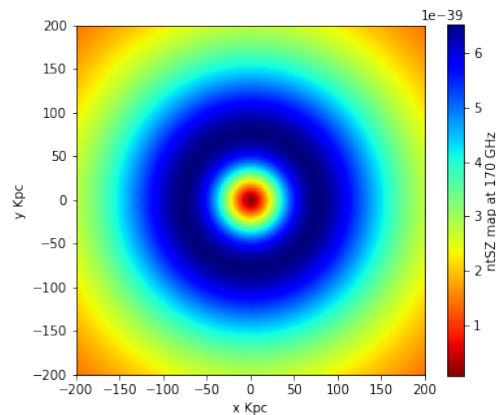


Figure 3.6: ntSZ map at 170 GHz using same values of p_1 , A , B and γ as in 4.4

In fig.3.6 the thermal pressure and hence X-ray observations enter via equation 3.12 Using the above we can prepare the total SZ map as a simple addition of these effects and check this simulated data against the real observation to constrain the non-thermal parameters p_1 , A , B and γ

$$SZ_{tot} \approx thSZ + ntSZ \quad (3.14)$$

Using simulations of ntSZ at different frequencies we will show how we can infer the parameters p_1 , A , B and γ by simulating total SZ at different frequencies.

Chapter 4

SZ parameter estimation

Here we demonstrate the use of SZ pack to estimate parameter using the model described in 3.0.3 and 3.0.4. Subsets of the model parameters $\{\tau, T_{e,SZ}, \omega^{(1,2,3)}, \sigma^{(1,2,3)}, \kappa^{(1,2,3)}, \beta_{c,\parallel,SZ}, \beta_{c,\perp,SZ}^2\}$ can then be estimated from measurements of the SZ spectrum.

This estimation is done and suggested earlier in [Chluba, Switzer, et al. 2013](#), here we use SZ pack and MCMC ([Foreman-Mackey et al. 2013](#)) to demonstrate the use of library in parameter estimation.

We will conclude with how the non-thermal SZ parameters $\{p_1, A, B, \gamma\}$ can be estimated assuming a spectral index(α) from synchrotron studies of galaxy clusters and fitted electron density and temperature maps from X-ray observations.

4.1 Data

We use SZ data compiled by [Prokhorov et al. 2012a](#), where observation frequency channels are 150, 275, 600, 857 GHz With mean intensity and errors $\Delta I = 0.325 \pm 0.015, 0.21 \pm 0.077, 0.268 \pm 0.031, 0.097 \pm 0.019$. We assume that $\tau = 0.0138 \pm 0.0016$ is known from ([Prokhorov et al. 2012a](#)).

4.2 Models

4.2.1 Asymptotic Model:

Using the model used by Prokhorov described as below,

$$\frac{\Delta I}{I_0} \approx \tau \left[g_0(x) \frac{\langle kT_e \rangle}{m_e c^2} + g_1(x) \frac{\langle (kT_e)^2 \rangle}{m_e^2 c^4} + g_2(x) \frac{\langle (kT_e)^3 \rangle}{m_e^3 c^6} \right] \quad (4.1)$$

where g_0, g_1 and g_2 are the functions of frequency that represents Taylor expansion by [Challinor et al. 1998](#). Calling the coefficients of these spectral functions as ω_1, ω_2 and ω_3 , we take these as

parameters for MCMC analysis.

The variation in temperature can be captured by estimating $\sigma^2 = \langle (KT_e)^2 \rangle - \langle KT_e \rangle^2$, by fitting for the coefficients in 4.1 .

4.2.1.1 Results:

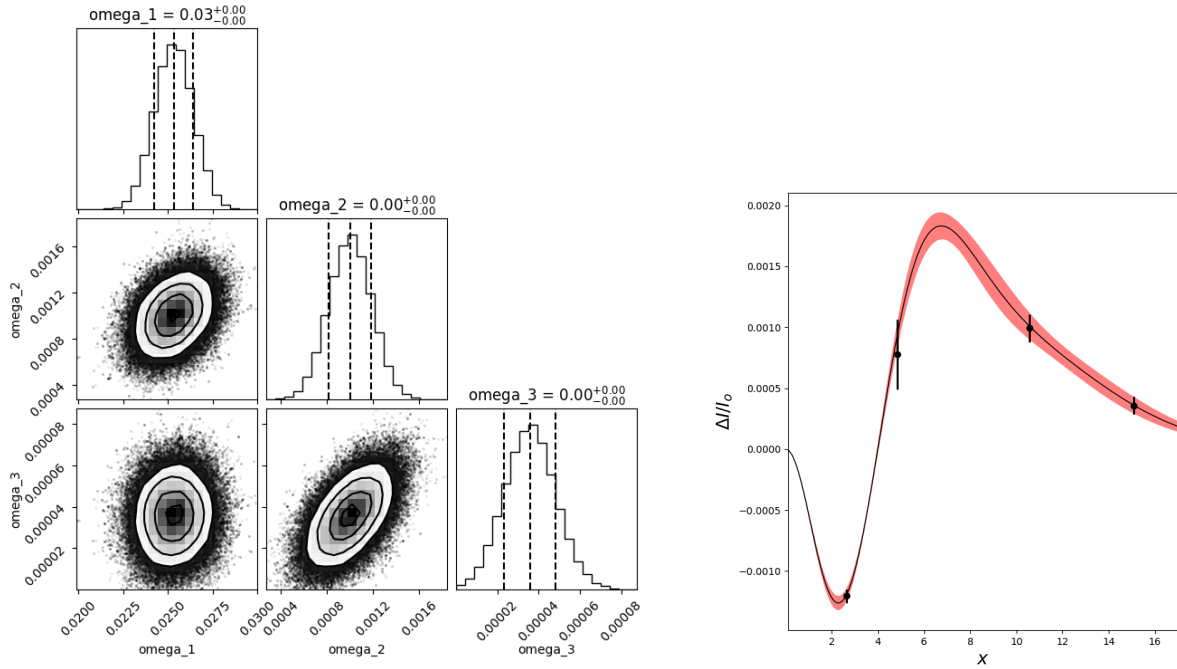


Figure 4.1: Left: Posterior distribution for Prokhorov's model after running the MCMC. Right: Best fit according to Prokhorov's model with 95 % confidence interval shown.

- We find the variation in temperature to be (9.5 ± 2.3) keV, that agrees with value of (9.5 ± 2.6) keV reported by [Prokhorov et al. 2012b](#)
- From X-Ray study by [Million et al. 2009](#) bullet cluster average temperature is reported to be 14.5 keV. Changing from moments defined above to temperature we have $T_e = (12.9 \pm 0.5) \text{ KeV}$ and $\omega^{(1)} \approx \sigma^2/T_e^2 = (0.5 \pm 0.3)$ for this model.

However at high temperature we can see from figure 4.2 calculated with SZpack that this Taylor series expansion approach breaks down and we cannot use this model. So this shows that we can use SZpack that can calculate these correction terms more accurately.

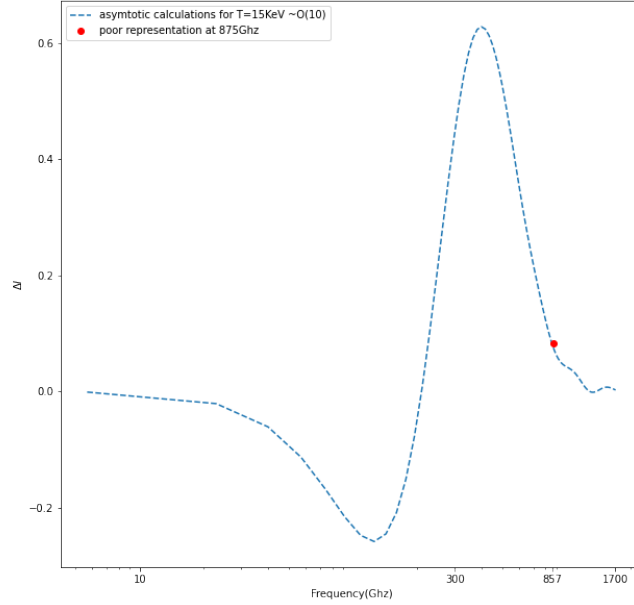


Figure 4.2: Poor representation of SZ signals using asymptotic approach, similar to Prokhorov's model.

4.2.2 Two-Temperature Model:

Now we can redo the analyses by [Chluba, Switzer, et al. 2013](#) to apply the model in [2.2.3](#).

- Parameters to be inferred are some reference T_e , a temperature difference ΔT , in the region with second temperature $T_e + \Delta T$ we take $f_\tau < 1$.
- Now we can calculate SZ signals from these two different regions separately i.e one temperature T_e and second with $T_e + \Delta T$ using SZpack that calculates the relativistic corrections as well.

4.2.2.1 Results:

Here we find $\omega^{(1)} = 0.8 \pm 0.5$

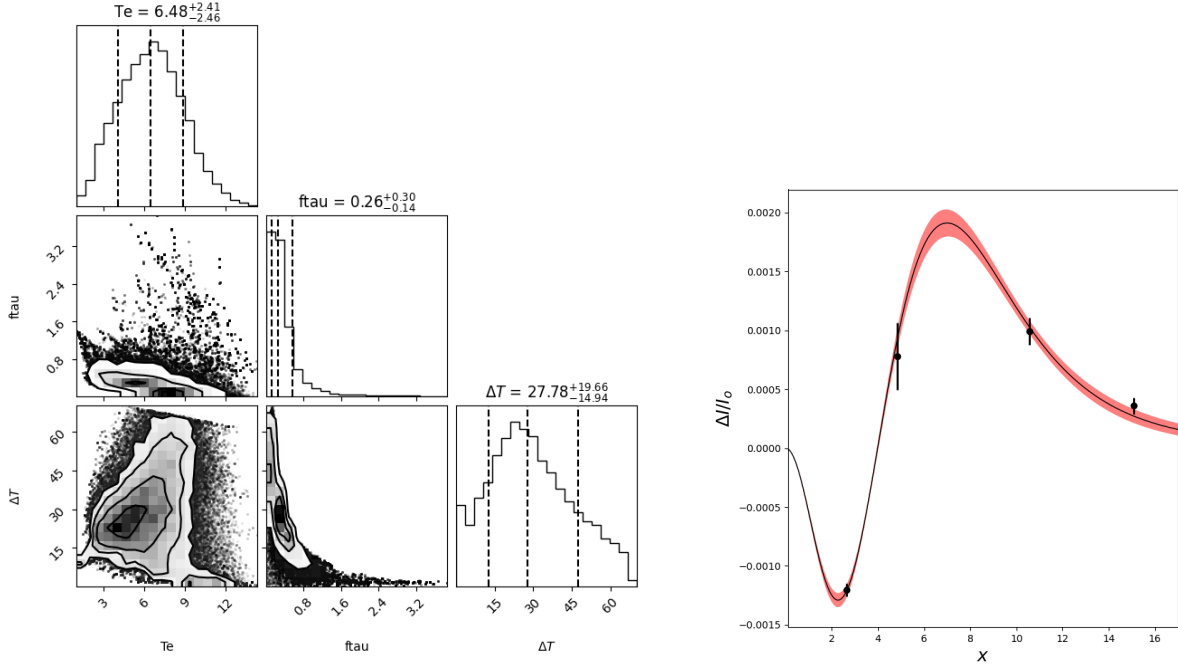


Figure 4.3: Left: Posterior distribution for model parameters for two-temperature model(cf., [Chluba, Switzer, et al. 2013](#)), on x-axis we have τ, f_τ and T_e . Right: Best model fit for two-temperature model.

4.3 Non-Thermal parameter estimation

Referring to equation 3.13 and eq.3.8 the spatial dependence of ntSZ can be calculated separately and taking the calculation along the diagonal element will save computational cost for running MCMC chain. We can write eq.3.13 more conveniently as,

$$\Delta I_\nu \approx \tau_{rel}(p_{min}, A, B, \gamma) * \tilde{g}(x; p_{min}) \quad (4.2)$$

For example we have modelled τ_{rel} as shown below fixing p_{min}, A, B and γ as before.

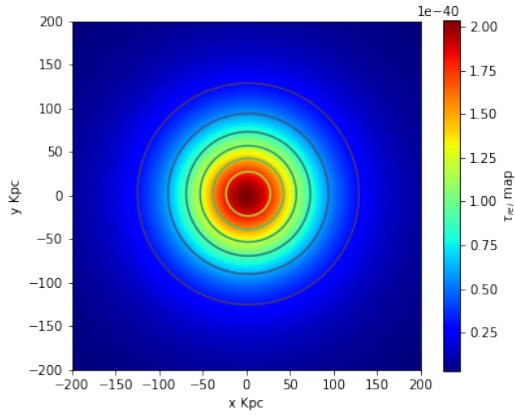


Figure 4.4: Relativistic optical-depth τ_{rel}

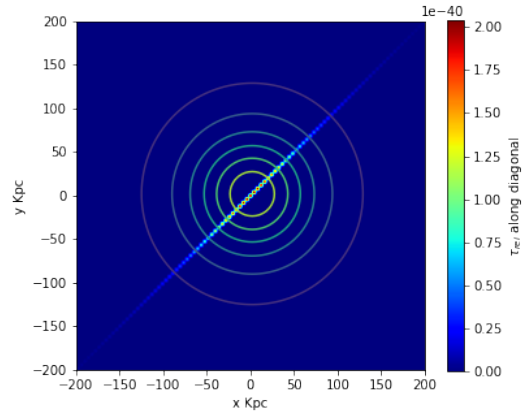


Figure 4.5: Calculations only in diagonally significant region

Now we have simulated the total SZ maps at different frequencies.

In fig.4.6 the complex features of SZ distortions are clearly seen when both the thermal and non-thermal populations are present in the galaxy clusters. At some particular map parameters can be constrained better, however that both depends upon the spatial and spectral variation of both effects.

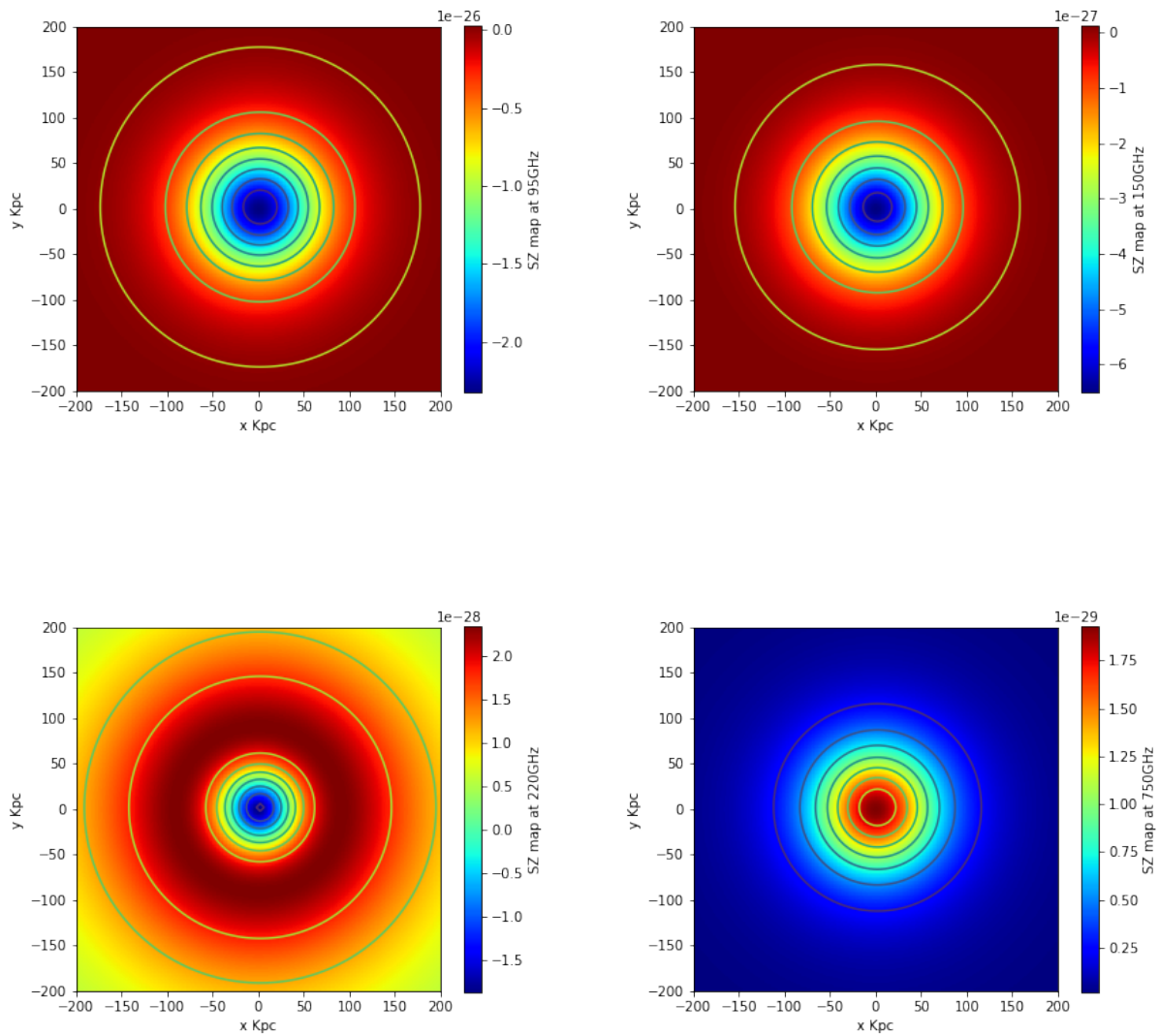


Figure 4.6: Total SZ signals at different frequencies

Chapter 5

Conclusions and Future Prospects

Here an SZ view of cluster gas physics is shown by, using an accurate description of SZ signals implied in SZpack, by preparing SZ maps .Discussion about various cluster models suggests it will be instrumental to study complex clusters with variable temperature and velocity moments.

Following that we prepared SZ maps using SZpack demonstrating its importance in studying cluster morphology.The importance of ntSZ signals are discussed and a way to calculate them is presented that will be fruitful in analysing the real observations.

5.1 Thermal SZ simulations of Bullet cluster:

Data:

Bullet Cluster is one of the most studied galaxy clusters. There have been several X-ray observations of Buller Cluster from which the X-ray surface brightness map and high fidelity temperature maps have been created (Datta et al. 2021 (in prep.)). Here, we have used the same X-Ray temperature map and fitted double-beta density profile from X-Ray surface brightness map. These two observable are used as input to predict the resultant thermal SZ signal for Bullet cluster at different frequencies.

Double-beta model fit values ($n \sim \sqrt{S_X}$)			
No.	Name	Value	error
1.	β	1.71495	$1.08524x10^{-1}$
2.	r_{c1}	1.07368'	$5.70285x10^{-2}$
3.	r_{c2}	2.96665'	$1.37319x10^{-1}$
4.	ratio	$9.56276x10^{-1}$	2.88163^{-2}
5.	norm	$1.78157x10^{-4}$	$3.18138x10^{-6}$
6.	const	$4.23959x10^{-6}$	$1.56013x10^{-7}$

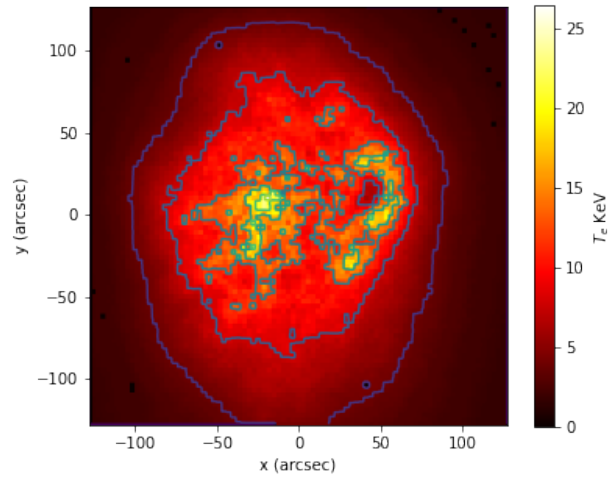


Figure 5.1: Temperature map from X-Ray observations

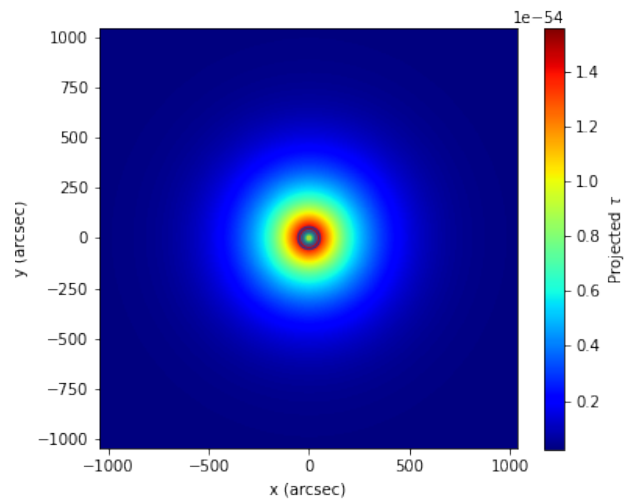


Figure 5.2: Optical depth τ from eq. 5.1

In table 5.1 the data is fitted with the double beta model¹ given by [Mohr et al. 1999](#) as,

$$S(r) = \text{norm} \left[\left(1 + (r/r_{c1})^2 \right)^{(-3\beta+0.5)} + \text{ratio} \left(1 + (r/r_{c2})^2 \right)^{(-3\beta+0.5)} \right] + \text{const} \quad (5.1)$$

5.1.1 Simulated tSZ map:

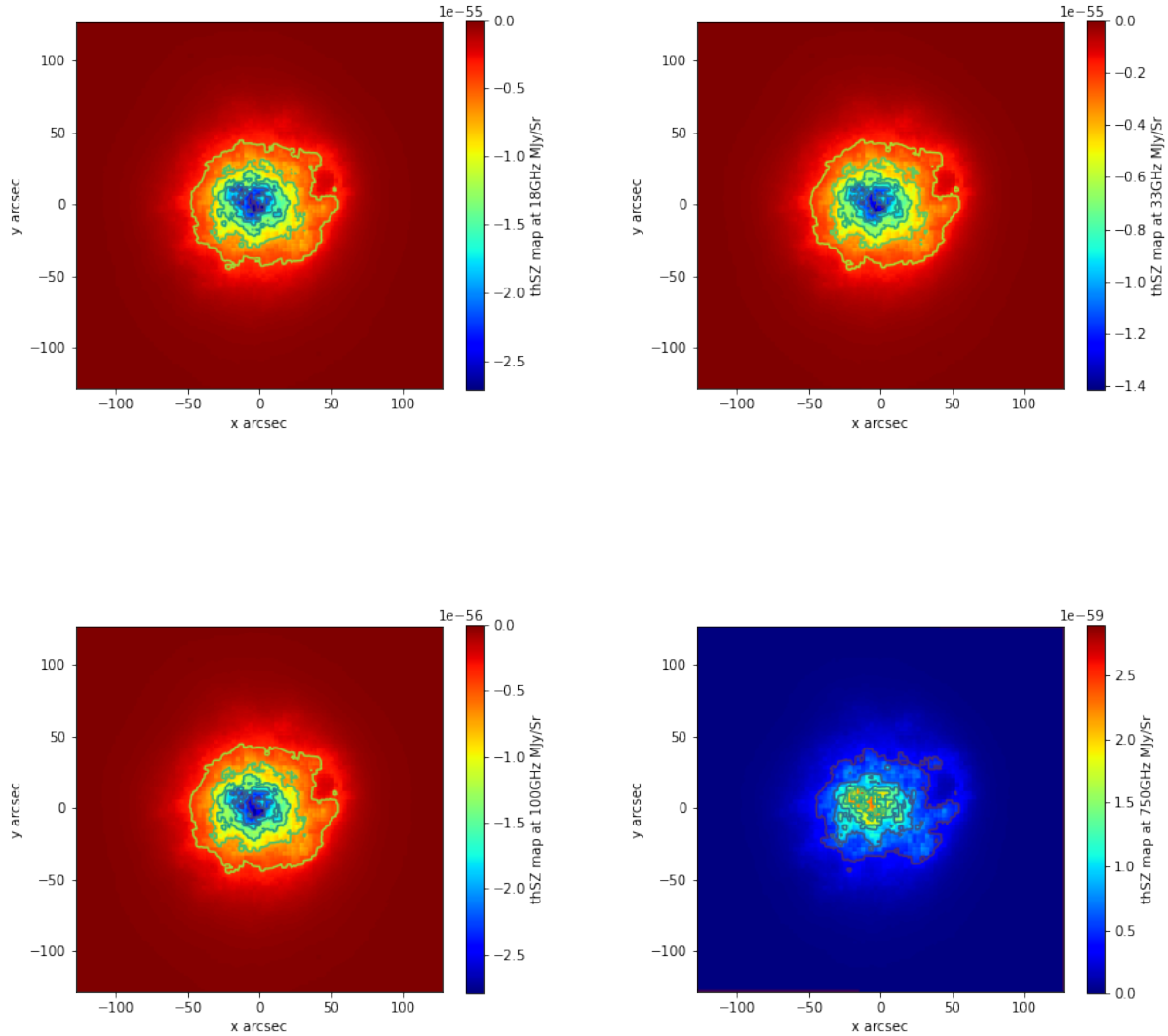


Figure 5.3: Simulated SZ signals for bullet cluster at frequencies from upper left to right 18,33,100 and 750 GHz respectively.

¹Himanshu would like to thank Majidul Rahman for the fitting

Note that in fig.5.3 because of approximation used in obtaining optical depth, the SZ intensity is only proportional to true distortion and these are not up to scale, however spectral and morphological features of bullet cluster are clear. And this allow us to compare this simulation with real observation of SZ distortions for e.g from Di Mascolo, Luca et al. 2019, and here we compare the same interferometric observation with our simulated map.

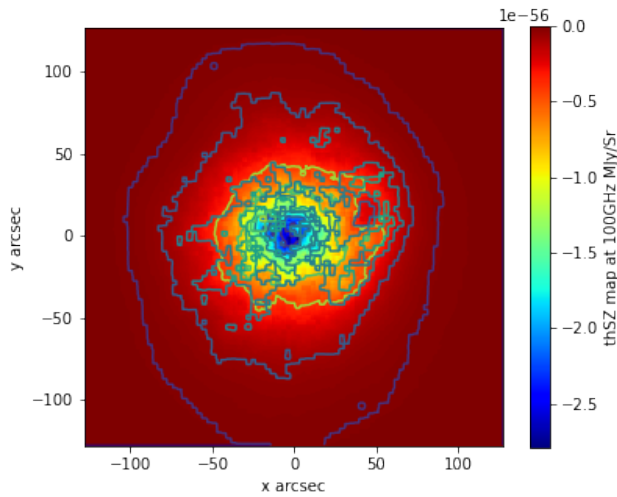


Figure 5.4: SZ map at 100 GHz with X-Ray temperature contours shown

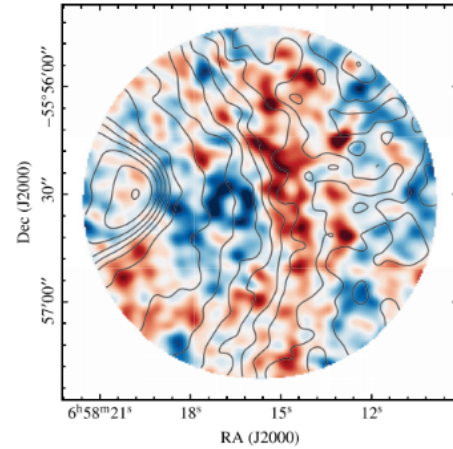


Figure 5.5: SZ observation of bullet cluster from Di Mascolo, Luca et al. 2019 at 100GHz

The interferometric observations are taken with ALMA+ACA at 100GHz. Comparing fig.5.4 and fig.5.5 we can clearly see the matching morphology of SZ signal even though the value we have is not absolute but frequency and spatial dependence is observable.

The applicability to estimate the parameters of thermal cluster physics is demonstrated using SZpack and MCMC and that can be applied to the simulated bullet cluster SZ signal given we have observational data for SZ distortion as well. But even without the real SZ observations the spectral features allows us relate the relative magnitude of cluster parameters such temperature moments.

Finally, we simulated ntSZ and total SZ signals in sec.4.3 at different frequencies showing the complex impact of thermal and non-thermal part on total signal, and a method to probe non-thermal cluster parameters is suggested using these complex 3 dimensional features so that our primary goal of probing non-thermal physics in galaxy clusters can be realized.

However, we have not yet applied these techniques to real SZ observation, for the future prospects,

though we can estimate the said parameter reducing the 2 dimensional data problem to 1 dimension as described in 3.2, however a complete picture of SZ effect is a 3 dimension problem, two in space and one in frequency, a more general approach that can take into account of the both spectral and spatial features at the same time would better constraint the parameters and furthers our understanding for these large scale structures called galaxy clusters and hence the Universe.

Bibliography

- Arnaud, M. (2008). Non thermal emission in clusters of galaxies. *Mem. Soc. Ast. It.*, 79, 170.
- Birkinshaw, M. (1999). The Sunyaev–Zel’dovich effect. *Physics Reports*, 310(2-3), 97–195. [https://doi.org/10.1016/s0370-1573\(98\)00080-5](https://doi.org/10.1016/s0370-1573(98)00080-5)
- Brunetti, G., & Jones, T. (2014). Cosmic rays in galaxy clusters and their non-thermal emission. *International Journal of Modern Physics D*, 23. <https://doi.org/10.1142/S0218271814300079>
- Bykov, A. M., Vazza, F., Kropotina, J. A., Levenfish, K. P., & Paerels, F. B. S. (2019). Shocks and Non-thermal Particles in Clusters of Galaxies. *Space Science Reviews*, 215(1), 14. <https://doi.org/10.1007/s11214-019-0585-y>
- Cavaliere, A., & Fusco-Femiano, R. (1978). The Distribution of Hot Gas in Clusters of Galaxies., 70, 677.
- Challinor, A., & Lasenby, A. (1998). Relativistic Corrections to the Sunyaev-Zeldovich Effect., 499(1), 1–6. <https://doi.org/10.1086/305623>
- Chluba, J., Nagai, D., Sazonov, S., & Nelson, K. (2012). A fast and accurate method for computing the Sunyaev-Zel’dovich signal of hot galaxy clusters. *Monthly Notices of the Royal Astronomical Society*, 426(1), 510–530. <https://doi.org/10.1111/j.1365-2966.2012.21741.x>
- Chluba, J., Switzer, E., Nelson, K., & Nagai, D. (2013). Sunyaev–Zeldovich signal processing and temperature–velocity moment method for individual clusters. *Monthly Notices of the Royal Astronomical Society*, 430(4), 3054–3069. <https://doi.org/10.1093/mnras/stt110>
- Colafrancesco, S., Marchegiani, P., & Palladino, E. (2002). The non-thermal Sunyaev–Zel’dovich effect in clusters of galaxies. *Astronomy Astrophysics*, 397(1), 27–52. <https://doi.org/10.1051/0004-6361:20021199>
- Di Mascolo, Luca, Mroczkowski, Tony, Churazov, Eugene, Markevitch, Maxim, Basu, Kaustuv, Clarke, Tracy E., Devlin, Mark, Mason, Brian S., Randall, Scott W., Reese, Erik D., Sunyaev, Rashid, & Wik, Daniel R. (2019). An ALMA+ACA measurement of the shock in the Bullet Cluster. *A&A*, 628, A100. <https://doi.org/10.1051/0004-6361/201936184>
- Enßlin, T. A., & Kaiser, C. R. (2000). Comptonization of the cosmic microwave background by relativistic plasma., 360, 417–430.
- Feretti, L., Fusco-Femiano, R., Giovannini, G., & Govoni, F. (2001). The giant radio halo in Abell 2163. *A&A*, 373(1), 106–112. <https://doi.org/10.1051/0004-6361:20010581>
- Foreman-Mackey, D., Hogg, D. W., Lang, D., & Goodman, J. (2013). emcee: The MCMC Hammer., 125(925), 306. <https://doi.org/10.1086/670067>
- Govoni, F., & Feretti, L. (2004). Magnetic field in clusters of galaxies. *Int. J. Mod. Phys. D*, 13, 1549–1594. <https://doi.org/10.1142/S0218271804005080>
- Govoni, F., Murgia, M., Feretti, L., Giovannini, G., Dolag, K., & Taylor, G. B. (2006). The intracluster magnetic field power spectrum in Abell 2255. *Astron. Astrophys.*, 460, 425. <https://doi.org/10.1051/0004-6361:20065964>

- Itoh, N., Kohyama, Y., & Nozawa, S. (1998). Relativistic Corrections to the Sunyaev-Zeldovich Effect for Clusters of Galaxies., *502*(1), 7–15. <https://doi.org/10.1086/305876>
- Lage, C., & Farrar, G. (2014). CONSTRAINED SIMULATION OF THE BULLET CLUSTER. *The Astrophysical Journal*, *787*(2), 144. <https://doi.org/10.1088/0004-637x/787/2/144>
- Malu, S., Datta, A., Colafrancesco, S., Marchegiani, P., Subrahmanyam, R., Narasimha, D., & Wieringa, M. (2017). Relativistic inverse Compton scattering of photons from the early universe. *Scientific Reports*, *7*. <https://doi.org/10.1038/s41598-017-17104-8>
- Million, E. T., & Allen, S. W. (2009). Chandra measurements of non-thermal-like X-ray emission from massive, merging, radio halo clusters. *Monthly Notices of the Royal Astronomical Society*, *399*(3), 1307–1327. <https://doi.org/10.1111/j.1365-2966.2009.15359.x>
- Mohr, J. J., Mathiesen, B., & Evrard, A. E. (1999). Properties of the Intracluster Medium in an Ensemble of Nearby Galaxy Clusters., *517*(2), 627–649. <https://doi.org/10.1086/307227>
- Mroczkowski, T., Nagai, D., Basu, K., Chluba, J., Sayers, J., Adam, R., Churazov, E., Crites, A., Di Mascolo, L., Eckert, D., & et al. (2019). Astrophysics with the Spatially and Spectrally Resolved Sunyaev-Zeldovich Effects. *Space Science Reviews*, *215*(1). <https://doi.org/10.1007/s11214-019-0581-2>
- Nelson, K., Lau, E. T., & Nagai, D. (2014). HYDRODYNAMIC SIMULATION OF NON-THERMAL PRESSURE PROFILES OF GALAXY CLUSTERS. *The Astrophysical Journal*, *792*(1), 25. <https://doi.org/10.1088/0004-637x/792/1/25>
- O'Dell, S. L., & Sartori, L. (1970). Low-Frequency Cutoffs in Synchrotron Spectra., *162*, L37. <https://doi.org/10.1086/180618>
- Palladino, E., Colafrancesco, S., & Marchegiani, P. (2002). Spatial features of non-thermal SZ effect in galaxy clusters. *616*. <https://doi.org/10.1063/1.1475660>
- Penzias, A. A., & Wilson, R. W. (1965). A Measurement of Excess Antenna Temperature at 4080 Mc/s., *142*, 419–421. <https://doi.org/10.1086/148307>
- Pizzo, R. F., & de Bruyn, A. G. (2009). Radio spectral study of the cluster of galaxies Abell 2255. *Astronomy Astrophysics*, *507*(2), 639–659. <https://doi.org/10.1051/0004-6361/200912465>
- Prokhorov, D. A., & Colafrancesco, S. (2012a). The first measurement of temperature standard deviation along the line of sight in galaxy clusters. *Monthly Notices of the Royal Astronomical Society: Letters*, *424*(1), L49–L53. <https://doi.org/10.1111/j.1745-3933.2012.01284.x>
- Prokhorov, D. A., & Colafrancesco, S. (2012b). The first measurement of temperature standard deviation along the line of sight in galaxy clusters. *Monthly Notices of the Royal Astronomical Society: Letters*, *424*(1), L49–L53. <https://doi.org/https://doi.org/10.1111/j.1745-3933.2012.01284.x>
- Rephaeli, Y. (1995a). Comptonization of the Cosmic Microwave Background: The Sunyaev-Zeldovich Effect. *Annual Review of Astronomy and Astrophysics*, *33*(1), 541–579. <https://doi.org/10.1146/annurev.aa.33.090195.002545>
- Rephaeli, Y. (1995b). Cosmic Microwave Background Comptonization by Hot Intracluster Gas., *445*, 33. <https://doi.org/10.1086/175669>
- Sazonov, S. Y., & Sunyaev, R. A. (1998). CMB radiation in the Direction of a Moving Cluster BF of Galaxies with Hot Gas: Relativistic Corrections. In J. Paul, T. Montmerle, & E. Aubourg (Eds.), *19th Texas Symposium on Relativistic Astrophysics and Cosmology* (p. 578).

- Sunyaev, R. A., & Zeldovich, I. B. (1980). Microwave background radiation as a probe of the contemporary structure and history of the universe., *18*, 537–560. <https://doi.org/10.1146/annurev.aa.18.090180.002541>
- Sunyaev, R. A., & Zeldovich, Y. B. (1970). The Spectrum of Primordial Radiation, its Distortions and their Significance. *Comments on Astrophysics and Space Physics*, *2*, 66.
- Sunyaev, R. A., & Zeldovich, Y. B. (1972). The Observations of Relic Radiation as a Test of the Nature of X-Ray Radiation from the Clusters of Galaxies. *Comments on Astrophysics and Space Physics*, *4*, 173.
- Vacca, V., Feretti, L., Giovannini, G., Govoni, F., Murgia, M., Perley, R. A., & Clarke, T. E. (2014). Spectral index image of the radio halo in the cluster Abell 520, which hosts the famous bow shock. *A&A*, *561*, A52. <https://doi.org/10.1051/0004-6361/201322504>
- Zeldovich, Y. B., & Sunyaev, R. A. (1969). The Interaction of Matter and Radiation in a Hot-Model Universe., *4*(3), 301–316. <https://doi.org/10.1007/BF00661821>